spin, it seems rather unlikely that a different value will apply for intermediate spin. The early work of Gammel *et al.*[10] for general spin provides some evidence (see particularly their Table 5) to support this idea. This leads to the possibility that for ferromagnetic Heisenberg interactions, the critical exponent γ has the same value irrespective of spin and the particular three-dimensional nearest-neighbor or finite-order equivalent-neighbor model considered.[45] Additional terms of the spin-$\frac{1}{2}$ equivalent-neighbor series would provide a useful means of testing this suggestion more thoroughly. The calculation of the required lattice constants[3] can be handled by electronic computer and it is hoped to extend the equivalent-neighbor series as far as the nearest-neighbor ones.

[45] This naturally suggests the similar behavior of other critical exponents. In the absence of detailed numerical evidence the assumption of such behavior might prove useful.

ACKNOWLEDGMENTS

We wish to thank Professor C. Domb, Dr. M. F. Sykes, Dr. D. S. Gaunt, and Dr. G. S. Joyce for many valuable discussions. Further, particular thanks are due to Dr. D. S. Gaunt for his comments on an earlier draft of this paper. We are indebted to the Science Research Council for research awards.

PHYSICAL REVIEW VOLUME 177, NUMBER 2 10 JANUARY 1969

Magnetic Symmetry and Antiferromagnetic Resonance in CoO

M. R. DANIEL* AND A. P. CRACKNELL
Department of Physics, University of Essex, Wivenhoe Park, Colchester, Essex, England
(Received 24 May 1968)

The irreducible corepresentations of the Shubnikov (magnetic) space group of ordered CoO (C_c2/c) have been deduced, and the magnon symmetries at various points in the Brillouin zone have been investigated. The antiferromagnetic resonance frequencies in CoO have been determined experimentally to be at 216.0, 221.0, and 248.0 cm^{-1} (each $\pm 0.2\%$). These results are compared with the neutron-scattering results and postulated magnon dispersion relations of Sakurai, Buyers, Cowley, and Dolling. It is suggested that the exchange constants J_1 and J_2 are about one order of magnitude smaller than previously assumed.

1. INTRODUCTION

AT high temperatures CoO assumes the NaCl structure. Below its Néel temperature antiferromagnetic CoO suffers a small tetragonal distortion and both a single-spin-axis structure and a multi-spin-axis structure have been proposed for the orientations of the spins. Antiferromagnetic resonance frequencies for CoO were calculated by Tachiki[1] and some experimental work has been done by Milward.[2] Neutron-scattering measurements have recently been performed both above and below the Néel temperature by Sakurai *et al.*[3]

2. COREPRESENTATIONS OF ANTIFERROMAGNETIC CoO STRUCTURE

In its paramagnetic state CoO assumes the NaCl structure so that the Co^{2+} ions form a fcc lattice. (See Fig. 1.) There have been two alternative suggestions concerning the arrangement of the spins in CoO at low temperatures. Below the Néel temperatures CoO is no longer exactly cubic but acquires a small tetragonal distortion. According to Shull *et al.*[4] and Roth[5] the spins are aligned in ferromagnetic sheets parallel to (111) planes with alternate signs in successive sheets. The actual spin direction was claimed to be in the $[11\bar{7}]$ direction and therefore at an angle of 11° 30′ to the z axis.[5] It is clear that such an orientation of the spins is not compatible with the retention of tetragonal symmetry, and an alternative multi-spin-axis structure for

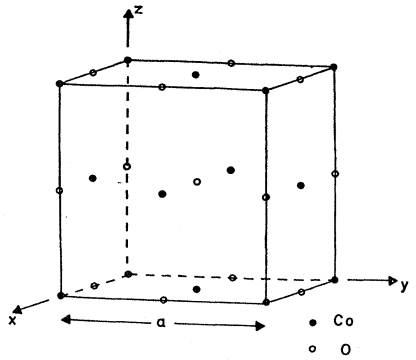

FIG. 1. The structure of paramagnetic CoO (NaCl structure).

* Present address: Westinghouse Electric Corp., Research Laboratories, Churchill Borough, Pittsburgh, Pa. 15235.

[1] M. Tachiki, J. Phys. Soc. Japan **19**, 454 (1964).

[2] R. C. Milward, Phys. Letters **16**, 244 (1965).

[3] J. Sakurai, W. J. L. Buyers, R. A. Cowley, and G. Dolling, Phys. Rev. **167**, 510 (1968).

[4] C. G. Shull, W. A. Strauser, and E. O. Wollan, Phys. Rev. **83**, 333 (1951).

[5] W. L. Roth, Phys. Rev. **110**, 1333 (1958).

the spin system in CoO was suggested by van Laar.[6] However, the theoretical work of Kanamori[7] and the experiments of Saito *et al.*[8] have established that in addition to the tetragonal distortion there is an extra rhombohedral distortion along the direction which was the [111] axis of the cubic phase. The combined effect of these two distortions is to reduce the symmetry of the ordered CoO to monoclinic; this produces a crystallographic structure that is consistent with the single-spin-axis structure[4,5] but is apparently not consistent with the multi-spin-axis structure.[6,8] Saito *et al.*[8] performed a low-temperature x-ray diffraction experiment and showed that the crystallographic structure of ordered CoO could be described by imposing first a tetragonal distortion along the c axis followed by a rhombohedral distortion along one of the former three-fold axes of the cube. The combined effect of these two distortions is to produce a monoclinic crystal structure with parameters as follows (Saito *et al.*[8]):

$C2/m$ C_{2h}^3 2 CoO per cell.
Lattice constants (−150°C), $a=5.18_3$ Å, $b=3.01_5$ Å, $c=3.01_7$ Å, and $\beta=125°\ 33.8'$.

A convenient alternative expression is the following:

A slightly deformed NaCl-type structure, 4 CoO per cell.
Lattice constants (−150°C), $a=b=4.26_5$ Å, $c=4.21_7$ Å, $c/a=0.988_7$, and $\alpha=\beta=\gamma=89°\ 58.8'$.

The relationship between the monoclinic unit cell and the original cubic CoO structure is illustrated in Fig. 2. The magnetic unit cell is twice the size of the crystallographic unit cell determined by x-ray diffraction and the spin orientations are shown in Fig. 2.

The magnetic space group of the ordered antiferromagnetic structure is $C_c2/c(B_b2/b)$, in the notation of

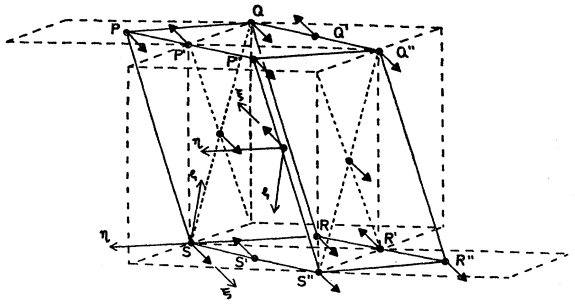

FIG. 2. The monoclinic unit cell of antiferromagnetic CoO related to its paramagnetic structure. $PQRSP'Q'R'S'$ is the crystallographic unit cell (Ref. 8) and $PQRSP''Q''R''S''$ is the magnetic unit cell.

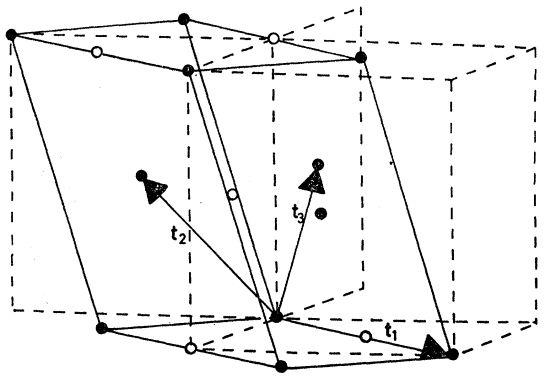

FIG. 3. The basic vectors $\mathbf{t}_1$, $\mathbf{t}_2$, and $\mathbf{t}_3$ of one sublattice of the black and white Bravais lattice of antiferromagnetic CoO.

Shubnikov and Belov,[9] which is a type-IV magnetic space group,[10] that is, a space group based on a black and white Bravais lattice. The symmetry elements of this magnetic space group can be simply obtained from the symmetry elements of the x-ray crystallographic space group $C2/m$ by adding the element $\theta\{E|\tau\}$, where θ is the operation of time inversion. The symmetry operations are therefore

$$\mathbf{M}=\{E|0\},\ \{C_{2b}|\tau\},\ \{I|0\},\ \{\sigma_{db}|\tau\},\ \theta\{E|\tau\},\ \theta\{C_{2b}|0\},\ \theta\{I|\tau\},\ \theta\{\sigma_{db}|0\}. \quad (1)$$

Here C_{2b} is a rotation through π about the $[1\bar{1}0]$ direction of the former cube and τ is a translation of $(\frac{1}{2}a\mathbf{i}+\frac{1}{2}a\mathbf{j})$, where $\mathbf{i}$, $\mathbf{j}$, and $\mathbf{k}$ are unit vectors in the x, y, and z directions in Fig. 1. For the paramagnetic phase in which the Co^{2+} ions form a fcc lattice one could choose basic vectors $\mathbf{t}_1$, $\mathbf{t}_2$, and $\mathbf{t}_3$ of the Bravais lattice where

$$\begin{aligned}\mathbf{t}_1&=(\tfrac{1}{2}a,\tfrac{1}{2}a,0),\\ \mathbf{t}_2&=(0,-\tfrac{1}{2}a,\tfrac{1}{2}a),\\ \mathbf{t}_3&=(-\tfrac{1}{2}a,0,\tfrac{1}{2}a).\end{aligned} \quad (2)$$

The basic vectors for one of the sublattices of the ordered antiferromagnetic phase of CoO can be taken to be

$$\begin{aligned}\mathbf{t}_1&=(a,b,0),\\ \mathbf{t}_2&=(0,-\tfrac{1}{2}b,\tfrac{1}{2}c),\\ \mathbf{t}_3&=(-\tfrac{1}{2}a,0,\tfrac{1}{2}c),\end{aligned} \quad (3)$$

where if we put $a=b=c$, since the distortion is very small, $\mathbf{t}_2$ and $\mathbf{t}_3$ are the same as in Eq. (2) but $\mathbf{t}_1$ has been doubled. (See Fig. 3.) The reciprocal lattice vectors that satisfy $\mathbf{g}_i\cdot\mathbf{t}_j=2\pi\delta_{ij}$ are given by

$$\begin{aligned}\mathbf{g}_1&=2\pi(1/2a,1/2b,1/2c),\\ \mathbf{g}_2&=2\pi(1/a,-1/b,1/c),\\ \mathbf{g}_3&=2\pi(-1/a,1/b,1/c),\end{aligned} \quad (4)$$

[6] B. van Laar, Phys. Rev. **138**, A584 (1965).
[7] J. Kanamori, Progr. Theoret. Phys. (Kyoto) **17**, 177 (1956); **17**, 197 (1956).
[8] S. Saito, K. Nakahigashi, and Y. Shimomura, J. Phys. Soc. Japan **21**, 850 (1966).
[9] A. V. Shubnikov and N. V. Belov, *Colored Symmetry* (Pergamon Press, Inc., New York, 1964).
[10] A. P. Cracknell, Progr. Theoret. Phys. (Kyoto) **33**, 812 (1965); C. J. Bradley and A. P. Cracknell, *ibid.* **36**, 648 (1966).

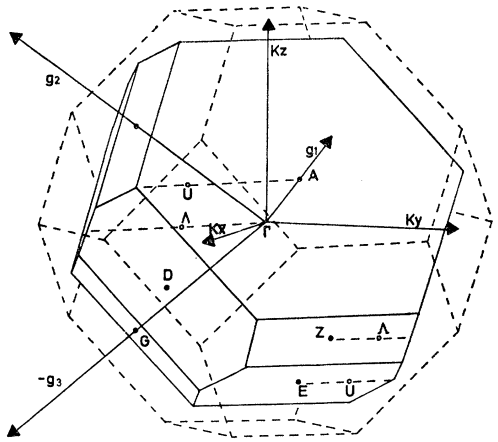

FIG. 4. The BZ of antiferromagnetic CoO; the paramagnetic BZ is shown in broken lines.

TABLE I. Magnetic little co-group of antiferromagnetic CoO. $\mathbf{k}$ is referred to $\mathbf{g}_1$, $\mathbf{g}_2$, and $\mathbf{g}_3$ given by Eq. (4) and $\bar{M}^{\mathbf{k}}$ is given by Eq. (5). Only the rotational parts of the space-group elements are given; see Eq. (1).

Point or line	$\mathbf{k}$	$\bar{G}^{\mathbf{k}}$	$\{E\|-\tau\}\bar{G}_I{}^{\mathbf{k}}$
Γ	(0,0,0)	$E, C_{2b}, I, \sigma_{db}$	$E, C_{2b}, I, \sigma_{db}$
A	$(\frac{1}{2},0,0)$	$E, C_{2b}, I, \sigma_{db}$	$E, C_{2b}, I, \sigma_{db}$
Z	$(\frac{1}{2}, -\frac{1}{2}, -\frac{1}{2})$	$E, C_{2b}, I, \sigma_{db}$	$E, C_{2b}, I, \sigma_{db}$
E	$(\frac{1}{2}, -\frac{1}{2}, -\frac{1}{2})$	$E, C_{2b}, I, \sigma_{db}$	$E, C_{2b}, I, \sigma_{db}$
G	$(0, 0, -\frac{1}{2})$	E, I	E, I
D	$(\frac{1}{2}, 0, -\frac{1}{2})$	E, I	E, I
Δ	$(0, \alpha, -\alpha)$[a] $(1, -1+\alpha, -\alpha)$[b]	E, C_{2b}	I, σ_{db}
U	$(\frac{1}{2}, \alpha, -\alpha)$[c] $(\frac{1}{2}, -1+\alpha, -\alpha)$[d]	E, C_{2b}	I, σ_{db}
B	(α,β,β)	E, σ_{db}	I, C_{2b}

[a] $0<\alpha\leqslant\frac{11}{32}$.
[b] $\frac{11}{32}\leqslant\alpha<\frac{1}{2}$.
[c] $0<\alpha\leqslant\frac{5}{16}$.
[d] $\frac{5}{16}\leqslant\alpha<\frac{1}{2}$.

where we can again in practice put $a=b=c$ because the distortion from cubic dimensions is very small.

Using $\mathbf{g}_1$, $\mathbf{g}_2$, and $\mathbf{g}_3$ given by Eq. (4), the magnetic Brillouin zone (BZ) can be constructed; this is illustrated in Fig. 4. In Fig. 4 we have put $a=b=c$ and show the antiferromagnetic BZ inside the paramagnetic fcc BZ; $\mathbf{g}_2$ and $\mathbf{g}_3$ of Eq. (4) are the same as would be obtained using Eq. (2), while $\mathbf{g}_1$ is half of the corresponding $\mathbf{g}_1$ for the cubic phase. The volume of the antiferromagnetic BZ is thus half of the volume of the BZ of the cubic phase. Therefore, in general, the zone boundaries will be closer to Γ than is shown by Fig. 4 of Sakurai *et al.*[3] In terms of the reduced wave vector ζ in Fig. 4 of Sakurai *et al.* the phonon BZ boundaries in the [001], [110], and [111] directions for $\mathbf{k}=(2\pi/a)(0,0,\zeta)$, $\mathbf{k}=(2\pi/a)(\zeta,\zeta,0)$, and $\mathbf{k}=(2\pi/a)(\zeta,\zeta,\zeta)$ occur at $\zeta=1.0$, 0.75, and 0.5, respectively. For the magnetic BZ shown in our Fig. 4, the boundaries are at $\zeta=0.75$ in the [001] direction, at $\zeta=0.375$ in the [110] direction, and at $\zeta=0.25$ in the [111] direction. Because [111] is along the direction of $\mathbf{g}_1$ the magnon dispersion curves along [111] from $\zeta=0$ to $\zeta=0.5$ should be symmetrical about $\zeta=0.25$. The behavior of the magnon branches along [001] for $\zeta>0.75$ and along [110] for $\zeta>0.375$ is more complicated because these are not along the direction of a reciprocal lattice vector. The six directions which were [110], [011], [101], [1$\bar{1}$0], [10$\bar{1}$], and [0$\bar{1}$1] in the cubic phase and which cut the BZ boundaries at a distance of $\frac{3}{4}\sqrt{2}(2\pi/a)$ from Γ in the cubic phase are now different and cut the BZ boundaries at different distances from Γ. If we ignore the distortions and put $a=b=c$ again, then [110], [011], and [101] cut the BZ boundary at $\frac{3}{8}\sqrt{2}(2\pi/a)$ from Γ, while [1$\bar{1}$0], [10$\bar{1}$], and [0$\bar{1}$1] cut the BZ boundary at $\frac{11}{16}\sqrt{2}(2\pi/a)$ from Γ. There will thus be different dispersion curves for the magnon frequency ν against $\mathbf{k}$ in these directions. Thus if one has a multi-domain sample, these curves will be superposed; this might explain the smudging of the magnon bands seen by Sakurai *et al.* A multi-domain structure can exist below the Néel temperature even in a crystal which is, crystallographically speaking, a single crystal because as the crystal is cooled below its Néel temperature there is a choice of four equivalent directions, [111], [$\bar{1}$11], [1$\bar{1}$1], and [11$\bar{1}$], for the normal to the ferromagnetic sheets. In different parts of the crystal a different one of these directions might be chosen so that one obtains a crystal that magnetically has a domain structure while being crystallographically a single crystal. The special points and lines of symmetry in this magnetic BZ are shown in Fig. 4 and the elements of the magnetic little co-group $\bar{M}^{\mathbf{k}}$ are given in Table I. We may write $\bar{M}^{\mathbf{k}}$ as

$$\bar{M}^{\mathbf{k}}=\bar{G}^{\mathbf{k}}+\theta\bar{G}_I{}^{\mathbf{k}}, \tag{5}$$

where $\bar{G}^{\mathbf{k}}$ consists of those unitary (uncolored) elements of the space group that send $\mathbf{k}$ into $+\mathbf{k}+\mathbf{K}_0$ and where $\theta\bar{G}_I{}^{k}$ consists of those antiunitary (colored) elements of the space group that send $\mathbf{k}$ into $-\mathbf{k}+\mathbf{K}_0$, where $\mathbf{K}_0$ is a vector of the reciprocal lattice.[11]

We now seek to determine the irreducible corepresentations of the magnetic little group of $\mathbf{k}$ for each of the points and lines of symmetry in the BZ. For the relevant theory we refer to the recent review article of Bradley and Davies[12]; we shall use their notation. The unitary subgroup of the magnetic space group C_c2/c (B_b2/b) is $C2/c$ $(B2/b)(C_{2h}{}^6)$ and the irreducible representations of the unitary subgroup can be determined from the tables of Faddeyev[13] or Kovalev.[14] Alternatively, since $C2/c$ is a relatively simple space group, it is probably just as easy to evaluate these irreducible representations *ab initio*. In Table II we give the

[11] J. O. Dimmock and R. G. Wheeler, Phys. Rev. **127**, 391 (1962).
[12] C. J. Bradley and B. L. Davies, Rev. Mod. Phys. **40**, 359 (1968).
[13] D. K. Faddeyev, *Tables of the Principal Unitary Representations of Federov Groups* (Pergamon Press, Inc., New York, 1964).
[14] O. V. Kovalev, *Irreducible Representations of the Space Groups* (Gordon and Breach, Science Publishers, Inc., New York, 1965).

TABLE II. Irreducible corepresentations of antiferromagnetic CoO. In the first column we label the irreducible representations of $\bar{G}^{\mathbf{k}}$ in the Mulliken notation and also, where possible, in the notation of Koster *et al.* (Ref. 16). In the final column we state whether the corepresentations of $\bar{M}^{\mathbf{k}}$ belong to case (a), case (b), or case (c).

Γ: $\mathbf{k}=(0,0,0)$		$\{E\|0\}$	$\{C_{2b}\|\tau\}$	$\{I\|0\}$	$\{\sigma_{db}\|\tau\}$	Coreps.
A_g	Γ_1^+	1	1	1	1	a
A_u	Γ_1^-	1	1	−1	−1	a
B_g	Γ_2^+	1	−1	1	−1	a
B_u	Γ_2^-	1	−1	−1	1	a

A: $\mathbf{k}=(\frac{1}{2},0,0)$; E: $\mathbf{k}=(\frac{1}{2},-\frac{1}{2},-\frac{1}{2})$

		$\{E\|0\}$	$\{E\|\mathbf{t}_1\}$	$\{\sigma_{db}\|\tau\}$ $\{\sigma_{db}\|-\tau\}$	$\{I\|0\}$ $\{I\|\mathbf{t}_1\}$	$\{C_{2b}\|\tau\}$ $\{C_{2b}\|-\tau\}$	Coreps.
E	A_1	2	−2	0	0	0	a
	E_1						

Z: $\mathbf{k}=(1,-\frac{1}{2},-\frac{1}{2})$

$\bar{M}^{\mathbf{k}}$ for Z is direct product of $\bar{M}^{\mathbf{k}}$ for Γ with $(\{E|0\}+\{E|\mathbf{t}_i\})$, $i=2$ or 3. The corepresentations all belong to case (a).

D: $\mathbf{k}=(\frac{1}{2},0,-\frac{1}{2})$

$\bar{M}^{\mathbf{k}}$ = direct product of $(\{E|0\}+\{E|\mathbf{t}_i\})$, $i=1$ or 3, with group below:

		$\{E\|0\}$	$\{I\|0\}$	Coreps
A_g	D_1^+	1	1	c
A_u	D_1^-	1	−1	

G: $\mathbf{k}=(0,0,-\frac{1}{2})$

$\bar{M}^{\mathbf{k}}$ = direct product of $(\{E|0\}+\{E|\mathbf{t}_3\})$ with group below:

		$\{E\|0\}$	$\{I\|0\}$	Coreps.
A_g	G_1^+	1	1	a
A_u	G_1^-	1	−1	a

Λ: $\mathbf{k}=(0,\alpha,-\alpha)$ or $(1,-1+\alpha,-\alpha)$

		$\{E\|0\}$	$\{C_{2b}\|\tau\}$	Coreps.
A	Λ_1	1	1	a
B	Λ_1	1	−1	a

U: $\mathbf{k}=(\frac{1}{2},\alpha,-\alpha)$ or $(\frac{1}{2},-1+\alpha,-\alpha)$

		$\{E\|0\}$	$\{C_{2b}\|-\tau\}$	Coreps.
A	U_1	1	i	a
B	U_2	1	$-i$	a

B: $\mathbf{k}=(\alpha,\beta,\beta)$

		$\{E\|0\}$	$\{\sigma_{db}\|\tau\}$	Coreps.
A	B_1	1	ξ	a
B	B_2	1	$-\xi$	a

$\xi=\exp(-i\mathbf{k}\cdot\tau)$

irreducible representations of the unitary subgroup $\bar{G}^{\mathbf{k}}$ for each of the points and lines of symmetry in the BZ and in the last column of each table we indicate whether the corepresentations of $\bar{M}^{\mathbf{k}}$ belong to cases (a), (b), or (c). Only the single-valued representations are included because they are the ones relevant to the magnons, and those single-valued representations that are not compatible with the representations of the translational group of the Bravais lattice are also omitted.

3. SINGLE-ION LEVELS AND MAGNONS IN CoO

A free Co^{2+} ion has the electronic structure $3d^7$ and its lowest term is a ^4F term.[15] The octahedral crystal field that a Co^{2+} ion in CoO sees is very similar to the field seen by a Co^{2+} ion substituted in MgO; in such a field the ^4F term splits[16,17] into an orbital triplet Γ_4 which is lowest, a triplet Γ_5 at 8470 cm^{-1} above Γ_4, and a singlet Γ_2 at 18 700 cm^{-1} above Γ_4 (see Fig. 5). These separations are so very much larger than the exchange splittings in antiferromagnetic CoO that we need only consider the Γ_4 level in investigating the magnons in CoO. The introduction of spin-orbit coupling leads to the splitting of these levels. The spin function belongs to $\mathfrak{D}^{3/2}$ or to Γ_8 of 432 (0), so that the splitting of the Γ_4 level by spin-orbit coupling is given by[16]

$$\Gamma_4\otimes\Gamma_8=\Gamma_6+\Gamma_7+2\Gamma_8. \tag{6}$$

In the ordered antiferromagnetic state the tetragonal distortion produces a crystalline field splitting of these cubic levels. Using the tables of Koster *et al.*,[16] we find that the levels Γ_6, Γ_7, and Γ_8 of 432 (0) split in 422 (D_4) according to (see Fig. 5)

$$\Gamma_6=\Gamma_6, \tag{7}$$

$$\Gamma_7=\Gamma_7, \tag{8}$$

and

$$\Gamma_8=\Gamma_6+\Gamma_7. \tag{9}$$

In considering crystalline electric field terms the tetragonal distortion is already small and therefore the splitting of the Γ_6 and Γ_8 cubic levels which it causes is very small; the small additional trigonal distortion along the [111] direction which reduces the structure to having the monoclinic symmetry of Fig. 2 causes no extra crystalline *electric* field splitting. The energy levels in Fig. 5(d) therefore represent the complete splitting

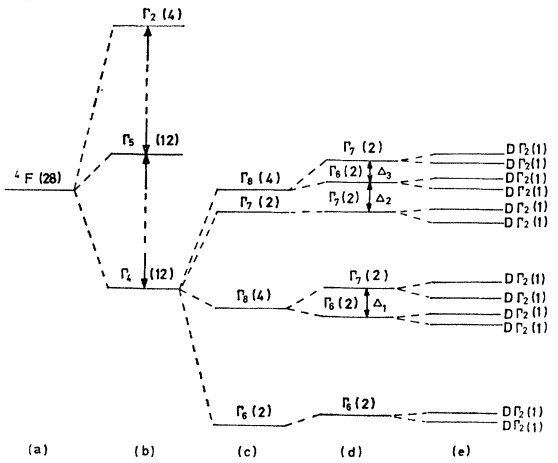

FIG. 5. The schematic splitting of the ^4F term of the Co^{2+} ion by various crystal fields and by spin-orbit coupling; (a) free atom, (b) cubic field 432 (0), (c) cubic field and spin-orbit coupling, (d) tetragonal field 422 (D_4), and (e) magnetic point group $2'/m'$.

[15] M. E. Lines, Phys. Rev. **137**, A982 (1965).

[16] G. F. Koster, J. O. Dimmock, R. G. Wheeler, and H. Statz, *Properties of the Thirty-Two Point Groups* (M.I.T. Press, Cambridge, Mass., 1963).

[17] W. Low, Phys. Rev. **109**, 256 (1958).

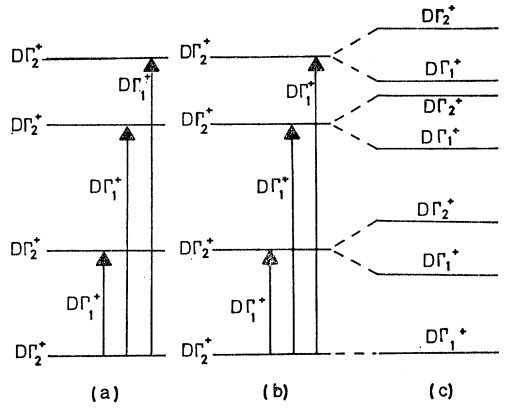

FIG. 6. Excitons and single-ion transitions (Co^{2+}, S odd); (a) and (b), single-ion levels and transitions for the two sublattices, (c) magnon or exciton levels at $\mathbf{k}=0$ derived from (a) and (b).

of the Γ_4 level due to the electric fields caused by all the distortions of the antiferromagnetic structure, Δ_1, Δ_2, Δ_3 being used to denote the splittings as indicated in Fig. 5(d); each of the levels in (d) still possesses twofold Kramers degeneracy. However, in the magnetically ordered state, although the monoclinic electric field is very small, there are large magnetic anisotropy and exchange fields and the twofold degeneracy of the Γ_6 and Γ_7 levels in Fig. 5(d) is lifted. From Eq. (1) we see that the point-group symmetry of the Co^{2+} ion consists of the elements E, I, θC_{2b}, and $\theta\sigma_{db}$ which constitute the magnetic point group $2'/m'$. Tables of the splitting of energy levels in crystalline fields, including both the electric field and the magnetic anisotropy and exchange fields, in a situation whose symmetry is described by any one of the magnetic point groups have been given in a recent article.[18] Using those tables, we see that each Γ_6 or Γ_7 level of Fig. 5(e) splits into two nondegenerate levels belonging to Γ_2 of the unitary subgroup or to the corepresentation $D\Gamma_2$ of $2'/m'$; see Fig. 5(e). The splitting of the Kramers doublets, Γ_6 or Γ_7 of Fig. 5(d), due to the anisotropy and exchange fields is probably much greater than the splitting due to the electrostatic effects of the tetragonal distortion.

We now study the combination of single-ion transitions on different sites to produce magnons or excitons which can propagate through the periodic structure of the crystal.[19] The transition operator $a^\dagger$, that generates a single-ion transition from the ground state belonging to the corepresentation $D\Gamma_g$ to an excited state belonging to the corepresentation $D\Gamma_e$, belongs to the corepresentation $D\Gamma_t$, where

$$D\Gamma_t = D\Gamma_e \otimes D\Gamma_g^*. \tag{10}$$

Since the Co^{2+} ion has an odd number of electrons, $D\Gamma_e$ and $D\Gamma_g$ are both the corepresentation $D\Gamma_2^+$ of $2'/m'$. For the unitary subgroup $\bar{1}(C_i)$ of $2'/m'$ we have[16]

$$\Gamma_2^+ \otimes \Gamma_2^+ = \Gamma_1^+. \tag{11}$$

Therefore, using the theory of the Kronecker products of irreducible corepresentations,[12,20] we find that

$$D\Gamma_t = D\Gamma_2^+ \otimes D\Gamma_2^+ = D\Gamma_1^+. \tag{12}$$

To combine the site-group corepresentations to form the space-group corepresentations we have the following rule[19]: If R is not in the site group $\chi(R)=0$ and if R is in the site group, then $\chi(R)$ is twice the character of R in the site group. Considering the unitary subgroups, we obtain the space-group representation Γ_r at $\mathbf{k}=0$ given by Table III and we see that Γ_r is reducible;

$$\Gamma_r = \Gamma_1^+ + \Gamma_2^+. \tag{13}$$

In terms of corepresentations of C_c2/c (B_b2/b) this means that the excitons or magnons at $\mathbf{k}=0$ in CoO derived from some single-ion transition belong to two nondegenerate case (a) corepresentations $D\Gamma_1^+$ and $D\Gamma_2^+$. That is, there is a Davydov splitting of the pair of magnons derived from each single-ion transition; see Fig. 6. Similar splittings occur in CoF_2 and NiF_2 but are not found, for example, in MnF_2.

TABLE III. Space-group exciton or magnon symmetries at $\mathbf{k}=0$ in CoO.

	$\{E\|0\}$	$\{C_{2b}\|\tau\}$	$\{I\|0\}$	$\{\sigma_{db}\|\tau\}$
Γ_r	2	0	2	0
		$\Gamma_r=\Gamma_1^+ + \Gamma_2^+$		

We seek to determine the symmetries of the magnons with various $\mathbf{k}$ vectors, i.e., to determine to which corepresentations the wave functions of the magnons belong. This can be done by studying the transformation properties of the magnon creation operators[19]

$$\alpha_{\downarrow\mathbf{k}}^\dagger = \frac{1}{\sqrt{(2SN)^{1/2}}}\{u_{\mathbf{k}} \sum_i \exp(i\mathbf{k}\cdot\mathbf{r}_i) S_i^- - v_k \sum_j \exp(i\mathbf{k}\cdot\mathbf{r}_j) S_j^-\} \tag{14}$$

and

$$\alpha_{\uparrow k}^\dagger = \frac{1}{\sqrt{(2SN)^{1/2}}}\{u_{\mathbf{k}} \sum_j \exp(i\mathbf{k}\cdot\mathbf{r}_j) S_j^+ - v_{\mathbf{k}} \sum_i \exp(i\mathbf{k}\cdot\mathbf{r}_i) S_i^+\}, \tag{15}$$

where i and j refer to the two sublattices. S^+ and S^- are

$$\begin{aligned} S^+ &= S_\xi + iS_\eta, \\ S^- &= S_\xi - iS_\eta, \end{aligned} \tag{16}$$

where ξ, ζ, and η form a right-handed orthogonal set of axes and ξ is along the direction of sublattice mag-

[18] A. P. Cracknell, Advan. Phys. **17**, 367 (1968).
[19] R. Loudon, Advan. Phys. **17**, 243 (1968).
[20] A. P. Cracknell, Progr. Theoret. Phys. (Kyoto) **38**, 1252 (1967).

TABLE IV. Symmetries of magnons in CoO.

Point or line	k	Magnon
Γ	(0,0,0)	Γ_1^+, Γ_2^+
A	$(\frac{1}{2},0,0)$	A_1
Z	$(1, -\frac{1}{2}, -\frac{1}{2})$	Z_1^+, Z_2^+
E	$(\frac{1}{2}, -\frac{1}{2}, -\frac{1}{2})$	E_1
G	$(0, 0, -\frac{1}{2})$	G_1^+, G_1^+
D	$(\frac{1}{2}, 0, -\frac{1}{2})$	(D_1^+, D_1^-)
Λ	$(0, \alpha, -\alpha)$[a]	Λ_1, Λ_2
	$(1, -1+\alpha, -\alpha)$[b]	
U	$(\frac{1}{2}, \alpha, -\alpha)$[c]	U_1, U_2
	$(\frac{1}{2}, -1+\alpha, -\alpha)$[d]	
B	(α,β,β)	B_1, B_2

[a] $0 < \alpha \leqslant \frac{11}{32}$.
[b] $\frac{11}{32} \leqslant \alpha < \frac{1}{2}$.
[c] $0 < \alpha \leqslant \frac{5}{16}$.
[d] $\frac{5}{16} \leqslant \alpha < \frac{1}{2}$.

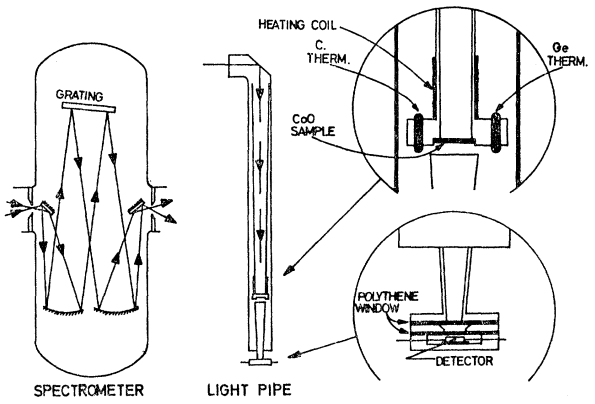

FIG. 7. Optical arrangement of far-infrared spectrometer and details of light pipe.

netization. We choose η along the twofold axis and this fixes ζ; ξ, ζ, and η are illustrated for each sublattice in Fig. 2. The effect of the symmetry operations on S^+ and S^- can easily be seen to be

$$\begin{aligned} ES^+ &= S^+, & ES^- &= S^-, \\ C_{2b}S^+ &= -S^-, & C_{2b}S^- &= -S^+, \\ IS^+ &= S^+, & IS^- &= S^-, \\ \sigma_{db}S^+ &= -S^-, & \sigma_{db}S^- &= -S^+. \end{aligned} \tag{17}$$

Therefore, using $\alpha_{\downarrow k}^\dagger$ and $\alpha_{\uparrow k}^\dagger$, the magnons can be assigned to the irreducible corepresentations of the magnetic little groups of C_c2/c; the results are given in Table IV. It can be seen that the magnon branches are nondegenerate everywhere except at the points A, D, and E. In particular we notice that there is a Davydov splitting of the magnon branches at Γ, Z, and G.

The initial state in the exciton creation process belongs to Γ_1^+ (see Fig. 6),[19] so that the magnons that are electric or magnetic dipole active are just the magnons which transform in the same way as the quantum-mechanical operator corresponding to the electric or magnetic dipole moments, i.e., as ξ, η, and ζ for electric-dipole transitions and L_ξ, L_η, and L_ζ for magnetic-dipole transitions. η belongs to Γ_1^- and ξ and ζ belong to Γ_2^- of the unitary subgroup of the magnetic little group at Γ; L_η belongs to Γ_1^+ and L_ξ and L_ζ belong to Γ_2^+. Selection rules that apply in the unitary subgroup will still be appropriate to the magnetic group[12,20] and therefore electric-dipole transitions are forbidden for all transitions from the ground state of Fig. 6(c) to any higher exciton level, whereas magnetic-dipole transitions will be allowed, with L_η for transitions to a $D\Gamma_1^+$ level and with L_ξ or L_ζ to a $D\Gamma_2^+$ level.

4. EXPERIMENTAL DETERMINATION OF ANTIFERROMAGNETIC RESONANCE FREQUENCIES

The absorption spectrum of CoO was investigated in the range 10–1000 cm^{-1} using a grating monochromator shown semischematically in Fig. 7. A Philips HPK high-pressure mercury lamp provided a continuous (frequency-wise) source for far-infrared radiation. A series of gratings blazed at 20° and ranging in spacing 936–13.9 lines/in. were used. As is usual in this technique, a series of filters consisting of powdered metal oxides dissolved in polyethylene sheets removed harmonics higher than the first from the radiation after diffraction by the gratings. The monochromatic radiation was channelled down an electroformed tapered copper pipe which acted as an optical condenser system by focusing the radiation on to the semiconductor detector. Three detectors were used: Cu-doped Ge in the range 1000–400 cm^{-1}, B-doped Ge in the range 400–80 cm^{-1}, and InSb in a 6-kG magnetic field (Putley detector) for the range 80–10 cm^{-1}. All detectors were operated in liquid helium and a phase-sensitive detection system was employed. A Princeton Applied Research Corp. H.R.8 lock-in amplifier provided the dc signal for displaying visually the absorption curve for CoO on a chart recorder. Figure 7 shows the CoO sample in the form of a disk 5 mm in diam located in the copper light pipe. By making a break in the pipe and enclosing it in an evacuated tube as shown, the sample could be thermally isolated from the surrounding helium bath. A combination of helium exchange gas and heating coil enabled transmission measurements to be done as a function of temperature from 4 to ~100°K. An Allen Bradley carbon resistance acted as thermometer and temperature sensing element for an electronic temperature controller using a Philbrick SP 656 operational amplifier. In this way any desired temperature could be maintained for extended periods while an absorption curve was recorded. The carbon resistance thermometer was calibrated against a Texas Instruments type 104 germanium thermometer. The polyethylene window at the bottom of the light pipe was found to provide a reliable vacuum seal in liquid helium. However, above 400 cm^{-1} its use was discontinued and measurements taken only at 4.2°K with liquid helium actually in the light pipe

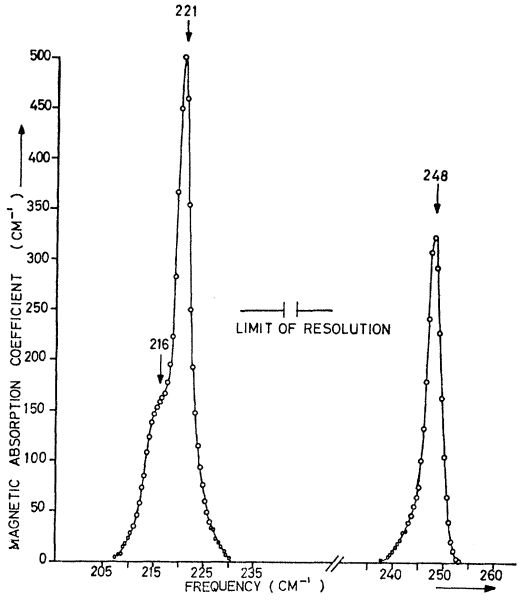

FIG. 8. Antiferromagnetic resonances in CoO at 4.2°K and zero applied magnetic field.

The intrinsic absorption spectra of polyethylene above 400 cm^{-1} complicated the interpretation of results sufficiently to discard its use as a window. Using a superconducting solenoid, transmission measurements were also made in a magnetic field of 40 kG.

Acting upon information from the Research Materials Information Center of Oak Ridge National Laboratory, a single-crystal boule of CoO was purchased from Marubeni Iida Co. Ltd. of Japan. The boule had been grown by a flame-fusion method from 99.5% pure starting material. It was examined by us by ultramicroscopy. Thin slices were observed to cause no scattering of visible light in transmission and we concluded that microscopic voids, cracks, or precipitates were absent. Measurements were made on disks cut from the boule oriented by the Laue back-reflection x-ray technique. The disks were, of course, single crystal and had a [100]-type axis normal to the plane of the disk; magnetically they were polydomain.

At 4.2°K all samples examined were found to be quite transparent from 10 to 200 cm^{-1}. No resonance at all was seen at 142.3 cm^{-1}, in disagreement with the results of Milward.[2] Above 200 cm^{-1} absorption became increasingly noticeable; at around 310 cm^{-1} the material was opaque. This is the onset of reststrahlen in CoO which continued up to 570 cm^{-1}. Above this frequency CoO was found to transmit only weakly up to 1000 cm^{-1} —the limit of the spectrometer—but with a broad hump of absorption extending from 625 to 730 cm^{-1}. This appears to be in qualitative agreement with the results of Marshall *et al.*[21] except their measurements did not extend below 250 cm^{-1}. Superimposed on the steadily increasing background absorption from 200 to 310 cm^{-1} were observed three resonances situated at 216.0, 221.0, and 248.0 cm^{-1} (accuracy about 0.2%). These are shown in Fig. 8.

An attempt was made to identify positively the resonances as resonant modes of the antiferromagnetic structure of CoO. The variation of resonance frequency was measured. Up to 70°K no shift was observed for any line; unfortunately at this temperature the lines had so broadened and the background absorption increased that further measurements above 70°K were frustrated. It is usually found that the frequency of an antiferromagnetic mode varies with temperature in the same way as the sublattice magnetization. However, with a Néel temperature of 292°K the sublattice magnetization of CoO at 70°K would show very little change from the saturation value at 0°K. Our results are, therefore, at least consistent with this. Additionally, a 40-kG magnetic field was found to have little effect (a slight narrowing and fall in intensity) on the resonances; we conclude they are due to magnetic-dipole active transitions between nondegenerate levels of the Co^{2+} ions.

We can compute the static magnetic susceptibility contributed to by the results in Fig. 8 using the standard Kramers-Kronig relation

$$\chi'(0)=\frac{2}{\pi}\int_0^\infty \frac{\chi''(\omega)d\omega}{\omega} \tag{18}$$

and the equation

$$\alpha(\omega)=8\pi^2 n\omega_0\chi''(\omega). \tag{19}$$

$\chi'(0)$ is the susceptibility at zero frequency or just $\chi_\perp$ in standard notation; $\chi''(\omega)$ is the complex part of the susceptibility at frequency ω. $\alpha(\omega)$ is the experimentally measured magnetic absorption coefficient in cm^{-1} with center frequency ω_0. The optical refractive index n was taken as a constant since magnetic-dipole transitions are weak in comparison with electric-dipole ones ($\sim 10^4$ less) and the change in n for CoO at resonance would only be a few percent. n was actually measurable from an incidental effect. Small oscillations were seen on the recorder output over the transparent range 100–10 cm^{-1} and were due to an optical interference effect within the CoO disk. Multiple reflections within the disk produced constructive and destructive interference effects which modulated the recorded signal to a small extent as the wavelength of the radiation was swept. From a knowledge of the disk thickness and the frequencies at which the oscillation maxima (or minima) occurred the refractive index was calculated to be 3.8 at around 50 cm^{-1}. Gielisse *et al.*[22] have calculated the refractive index for CoO as a function of frequency

[21] R. Marshall, S. S. Mitra, P. J. Gielisse, and J. N. Plendl, in *Proceedings of the Seventh International Conference on the Physics of Semiconductors, Paris, 1964* (Academic Press Inc., New York, 1964), p. 1101.

[22] P. J. Gielisse, J. N. Plendl, L. C. Mansur, R. Marshall, S. S. Mitra, R. Mykolajewycz, and A. Smakula, J. Appl. Phys. 36, 2446 (1965).

down to 250 cm^{-1}. Our value of 3.8 at 50 cm^{-1} is satisfactorily consistent with their value of 4.4 at 250 cm^{-1}. The integral for $\chi'(0)$ was approximated by a summation and each resonance divided into narrow strips to evaluate the summation. A correction was estimated for the effect of instrumental broadening of the lines in Fig. 8. The actual recorded resonance is the mathematical convolution of the true, unbroadened line shape with the instrumental response or resolution. The latter was obtained by recording the zero-order response from the diffraction grating in the spectrometer. The broadening is not large (10–15%) and was therefore allowed for approximately in the following way: $\chi_1'(0)$ was computed from a line shape obtained by convoluting the experimental line shapes with the spectrometer resolution. $\chi_1'(0)$ will be larger than $\chi_2'(0)$, computed directly from the experimental lines, by nearly the same as $\chi_2'(0)$ is larger than $\chi_3'(0)$, computed from the true unbroadened line shape.

We find the total contributions to $\chi'(0)$ from the resonances to be 11.8×10^{-5} emu. Uchida *et al.*[23] have measured the static susceptibility of CoO single crystals and find a value of 7.2×10^{-5} emu. The discrepancy between the values may in part be due to difficulties in measuring truly reliable absorption strengths. Compare the results, for example, of Aring and Sievers[24] and Allen[25] on antiferromagnetic UO_2. Clearly if there are any other magnetic-dipole transitions in CoO they must be either weak compared with our values or at much higher frequencies, or both, to give only small contributions to $\chi'(0)$. Milward[2] unfortunately gives no absorption strengths (except as relative ones) and so we cannot compute what contribution to $\chi'(0)$ his observed resonance would give. Accepting our results, it can only be very small.

5. MAGNON DISPERSION RELATIONS

We now seek to correlate the antiferromagnetic resonance results described in Sec. 4 with the neutron-scattering results of Sakurai *et al.*,[3] in order to determine the magnon dispersion relations for antiferromagnetic CoO.

An early calculation of the antiferromagnetic resonance frequencies in CoO by Tachiki[1] used the "old-fashioned" equation-of-motion methods and predicted two doubly degenerate frequencies at 192 and 554 cm^{-1} (5.76×10^{12} and 16.6×10^{12} Hz). These frequencies do not agree very closely with our measured frequencies of 216.0, 221.0, and 248.0 cm^{-1} and, moreover, it was found that an applied magnetic field (40 kG) did not reveal any degeneracies in our resonance frequencies. In Sec. 3 we described the combination of transitions between energy levels of single ions to produce excitons

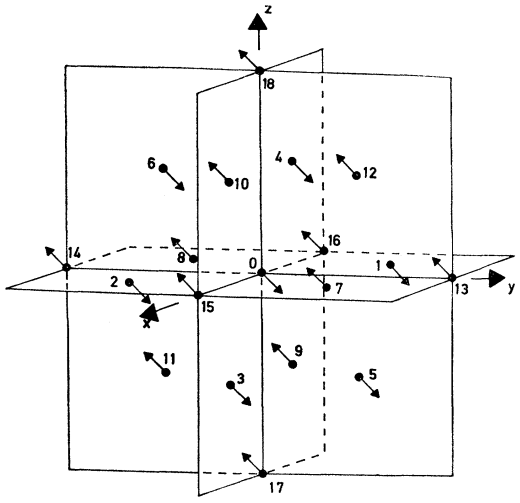

FIG. 9. The first and second nearest neighbors in CoO; 1–6 are nearest neighbors and are on the same sublattice as the ion at 0, 7–12 are also nearest neighbors to 0 but are on the opposite sublattice, 13–18 are second nearest neighbors to 0 and are also on the opposite sublattice.

or magnons. By using creation and annihilation operators corresponding to transitions between these states[15,19] we can obtain a theory of magnons or excitons that is related to transitions between the single-ion levels of the crystal and is less restricted than the method used by Tachiki.

We may use the Hamiltonian given by Sakurai *et al.*[3] which is essentially the same as the Hamiltonian used by Kanamori[7] and by Tachiki,[1]

$$\mathcal{H}=\sum_i(\lambda\mathbf{l}_i\cdot\mathbf{S}_i+c\mathbf{l}_{zi}^2)+\sum_{ij}J_{ij}\mathbf{S}_i\cdot\mathbf{S}_j, \tag{20}$$

where i refers to one sublattice and j refers to either sublattice, but $j\neq i$. This may be written in terms of the molecular-field single-ion energy level difference E_0, and the single-sublattice exciton creation operators $a_{\mathbf{k}}^\dagger$ and $b_{\mathbf{k}}^\dagger$ [19]:

$$\begin{aligned}\mathcal{H}=\sum_{\mathbf{k}}\{&[E_0+V_1(\mathbf{k})](a_{\mathbf{k}}^\dagger a_{\mathbf{k}}+b_{\mathbf{k}}^\dagger b_{\mathbf{k}})\\&+\tfrac{1}{2}V_1(\mathbf{k})(a_{\mathbf{k}}^\dagger a_{-\mathbf{k}}^\dagger+a_{\mathbf{k}}a_{-\mathbf{k}}+b_{\mathbf{k}}^\dagger b_{-\mathbf{k}}^\dagger+b_{\mathbf{k}}b_{-\mathbf{k}})\\&+V_2(\mathbf{k})(a_{\mathbf{k}}^\dagger b_{-\mathbf{k}}^\dagger+a_{\mathbf{k}}b_{-\mathbf{k}}+a_{\mathbf{k}}^\dagger b_{\mathbf{k}}+b_{\mathbf{k}}^\dagger a_{\mathbf{k}})\},\end{aligned} \tag{21}$$

where the single-ion transitions are between two levels of the same symmetry and

$$V_1(\mathbf{k})=\sum_{i'}V_{ii'}\exp[i\mathbf{k}\cdot(\mathbf{r}_i-\mathbf{r}_{i'})] \tag{22}$$

and

$$V_2(\mathbf{k})=\sum_j V_{ij}\exp[i\mathbf{k}\cdot(\mathbf{r}_i-\mathbf{r}_j)]. \tag{23}$$

In the notation of Eq. (20), $V_{ii'}$ is the exchange interaction $J_{iji}\mathbf{S}_i\cdot\mathbf{S}_j$ between two ions on the same sublattice and V_{ij} is the exchange interaction $J_{ij}\mathbf{S}_i\cdot\mathbf{S}_j$ between

[23] E. Uchida, N. Fukuoka, H. Kondoh, T. Takeda, Y. Nakazumi, and T. Nagamiya, J. Phys. Soc. Japan **19**, 2088 (1964).
[24] K. Aring and A. J. Sievers, J. Appl. Phys. **38**, 1496 (1967).
[25] S. J. Allen, J. Appl. Phys. **38**, 1478 (1967).

TABLE V. Magnon or exciton frequencies at Γ and E.

Γ: λ_- cm^{-1}	λ_+ cm^{-1}	Γ: λ_- 10^{12} Hz	λ_+ 10^{12} Hz	E: $\lambda_\pm$ cm^{-1}	E: $\lambda_\pm$ 10^{12} Hz
24	207	0.73	6.19	131	3.92
175	326	5.24	9.77	246	7.36
254	403	7.61	12.1	321	9.62
294	443	8.82	13.3	360	10.8
430	578	12.9	17.3	493	14.8
449	597	13.5	17.9	513	15.4
478	626	14.3	18.8	541	16.2
575	722	17.2	21.6	636	19.1
680	827	20.4	24.8	741	22.2
795	942	23.8	28.2	856	25.7
871	1020	26.1	30.5	932	27.9

two ions on different sublattices. The use of these $a_k^\dagger$ and $b_k^\dagger$ assumes that the orbital angular momentum of the Co^{2+} ion's electrons is completely quenched, which is known to be not quite true. However, this method is valuable for giving a particularly simple first approximation to the general features of the magnon or exciton dispersion relations. Having ascertained the gross features of the magnon-dispersion curves, the details can be refined later. The result of diagonalizing the Hamiltonian in Eq. (21) is given by[19]

$$\lambda_\pm(\mathbf{k})^2 = E_0^2 + 2E_0V_1(\mathbf{k}) \pm 2E_0V_2(\mathbf{k}). \quad (24)$$

Therefore, to determine the magnon frequencies from a given single-ion transition E_0, at any point in the BZ, it remains to determine $V_1(\mathbf{k})$ and $V_2(\mathbf{k})$. Of the 12 nearest neighbors of a Co^{2+} ion at 0 in Fig. 9 in the CoO structure, six are on the same sublattice and six are on the other sublattice; all the six second-nearest neighbors are on the other sublattice. If J_1 and J_2 are the first and second nearest-neighbor exchange constants then, considering $\mathbf{k}=0$, because this is the important wave vector for antiferromagnetic resonance,

$$V_1(0) = 6J_1S, \quad (25)$$

$$V_2(0) = 6J_1S + 6J_2S. \quad (26)$$

If E_0 is very much larger than either $V_1(\mathbf{k})$ or $V_2(\mathbf{k})$, Eq. (24) may be written as

$$\lambda_\pm(\mathbf{k}) = E_0 + V_1(\mathbf{k}) \pm V_2(\mathbf{k}). \quad (27)$$

Therefore the order of magnitude of the Davydov splitting at Γ is $2|V_2(0)|$. If one accepts the values of J_1 and J_2 given by Smart,[26] Kanamori,[7] or Sakurai *et al.*,[3] they all lead to a Davydov splitting of the order of 100–200 cm^{-1}. However, Figs. 4 and 5 of Sakurai *et al.*,[3] which illustrate the neutron-scattering results for the antiferromagnetic and paramagnetic states of CoO, respectively, appear to indicate that there is a broad "smudge" between 220 and 250 cm^{-1} (6.5×10^{12} and 7.5×10^{12} Hz) which is only present in the antiferromagnetic state and is almost $\mathbf{k}$-independent. It is very likely, since the three antiferromagnetic resonance frequencies that we have observed all lie within this range, that this smudge contains several magnon branches and that these magnon branches are relatively independent of $\mathbf{k}$. This would suggest, since in some directions at least the magnons become degenerate at the zone boundary, that $2|V_2(0)|$ is of the order of 30 cm^{-1} rather than 200 cm^{-1}. Moreover, if the values of J_1 and J_2 of Smart,[26] Kanamori,[7] and Sakurai *et al.*[3] are correct, then one would expect that the observed antiferromagnetic resonance frequencies reported in Sec. 4 would all be single members of separate pairs of Davydov-split pairs of magnon frequencies. Therefore, one would expect to see the other members of these pairs at about 240 ± 100 cm^{-1}, i.e., about 140 or 340 cm^{-1}. Such magnon frequencies have not been observed in our antiferromagnetic resonance experiments, nor are they consistent with the complete separation all over the BZ of the two sets of magnon branches of Sakurai *et al.*[3] This also supports the view that $2|V_2(0)|$, the Davydov splitting at Γ, is small, namely, of the order of 30 cm^{-1} rather than 200 cm^{-1} or so.

In Fig. 5(e) the 12 single-ion levels derived from the cubic Γ_4 level are shown. These levels are also shown in Fig. 7 of Sakurai *et al.*,[3] where, with the value of J_2 postulated by Sakurai *et al.*, each of these levels is separated from the next one by a few tens of wave numbers. Because of the closeness of the single-ion levels and because every single-ion transition will lead to a pair of excitons or magnons, one would expect there to be many more magnon branches than there are shown in the broken curves in Fig. 4 of Sakurai *et al.* Indeed one might expect not only the transitions from the lowest of these 12 levels but even some transitions between higher pairs of levels to lead to observable magnons (see, e.g., Lines[15] on CoF_2). For these 12 levels derived from Γ_4 neither L nor S is a good quantum number. One can only say that they all belong to the corepresentation $D\Gamma_2^+$ of the site group of the Co^{2+} ion site group (see Sec. 3).

If we use the single-ion levels given in Fig. 7 of Sakurai *et al.*[3] together with their values of J_1 and J_2, we can calculate the frequencies of those magnons derived from transitions out of the lowest level into any of the other 11 levels. At $\mathbf{k}=0$, using Eqs. (22), (23), and (25), we obtain the frequencies given in Table V. It will be noticed from Table V that within the range of the neutron-scattering experiments of Sakurai *et al.*,[3] i.e., from 0 to 18×10^{12} Hz, there are 14 calculated magnon frequencies at $\mathbf{k}=0$ and that these are widely distributed over this range. However, the only magnon frequencies actually observed experimentally by Sakurai *et al.* appear to be two smudges, one between 4.5×10^{12} and 5.5×10^{12} Hz and the other between 6.5×10^{12} and 7.5×10^{12} Hz. If one considers the antiferromagnetic resonance data of Milward[2] and the lines that we have reported in Sec. 4, then one might obtain a fit to four of the calculated lines by making some small adjustments to the parameters. But this

[26] J. S. Smart, *Effective Field Theories of Magnetism* (W. B. Saunders, Philadelphia, 1966).

still leaves many calculated lines in the regions that we have examined and found to be completely empty of resonance lines. This would seem to suggest that the energy-level splitting (Fig. 7 of Sakurai *et al.*) and the values of J_1 and J_2 deduced by Sakurai *et al.* are too large to fit the observed magnon frequencies.

We must also consider the $\mathbf{k}$ dependence of the magnon frequencies both theoretically and experimentally. As a typical point on the surface of the BZ we may take E. At E, $\mathbf{k}=\frac{1}{2}\mathbf{g}_1-\frac{1}{2}\mathbf{g}_2-\frac{1}{2}\mathbf{g}_3$ and $V_1(\mathrm{E})$ and $V_2(\mathrm{E})$ are given by

$$V_1(\mathrm{E})=-2J_1S \tag{28}$$

and

$$V_2(\mathrm{E})=0. \tag{29}$$

The magnon frequencies are therefore degenerate at E and are given in columns 5 and 6 of Table V. It seems, therefore, that the calculated magnon frequencies vary considerably more rapidly with $\mathbf{k}$ than the neutron-scattering results of Sakurai *et al.* seem to imply. For example, the second magnon branch in Table V is nondegenerate at Γ (174.6 cm^{-1} and 326.0 cm^{-1}) and is degenerate at E (245.5 cm^{-1}); therefore it has a width of approximately 150 cm^{-1} (approximately 4.5×10^{12} Hz). Such a magnon branch width is about four times that observed using neutron scattering.

6. CONCLUSION

We would suggest, in the light of the comments of Sec. 5, that the splitting of the levels in Fig. 5(d) by the crystal field due to the distortion and in Fig. 5(e) by the exchange field is small and also that J_1 and J_2 are small. By "small" we mean approximately one order of magnitude smaller than that used by Sakurai *et al.* This would mean that single-ion transitions between the ground state and the set of four levels would give rise to eight magnon frequencies within the range of 4.5×10^{12}–5.5×10^{12} Hz, i.e., within the lower smudge of Sakurai *et al.*[3] Transitions between the ground state and the higher set of six levels would give rise to 12 magnon frequencies within the range 6.5×10^{12}–7.5×10^{12} Hz, i.e., within the second smudge of Sakurai *et al.* In both smudges the magnon frequencies do not vary much (i.e., $<0.5\times10^{12}$ Hz) over the whole BZ. If there are as many magnon frequencies crammed into these relatively small regions as we have just suggested, it is quite likely that the neutron-scattering measurements would not be able to resolve them all and would simply produce a smudge as seen by Sakurai *et al.* The fact that we have resolved three antiferromagnetic frequencies within the higher smudge of Sakurai *et al.* would seem to favor our interpretation. However, we must admit that there are deficiencies in our interpretation, namely, (i) we have been unable to observe the resonance observed by Milward at 142.3 cm^{-1} which would fit nicely into the lower smudge of Sakurai *et al.* and would agree with our interpretation of the single-ion level scheme and our suggested values of J_1 and J_2; (ii) on the molecular field theory, small values of J_1 and J_2 would seem to be incompatible with the very high Néel temperature (292°K) of CoO; this difficulty could be avoided by postulating a large anisotropy field to go with the small exchange field (see, e.g., Kanamori[27]), but this would have the undesirable effect of producing large splittings in Fig. 5(e); (iii) we have not resolved anything like the large number of magnons that would appear in the interpretation just given (eight in the lower smudge and 12 in the upper smudge, not to mention other magnons arising from transitions between the other pairs of levels that do not involve the ground state at all).

Recent experiments of Ok and Mullen[28] have been interpreted as suggesting that there is no distortion from cubic symmetry in antiferromagnetic CoO. These authors claim that ordinary CoO is a mixture of two forms, one of which [CoO(I)] has the NaCl structure with ideal stoichiometry and perfect translational symmetry, while the other [CoO(II)] has the NaCl structure with half of its positive ion sites and half of its negative-ion sites vacant. However, it appears that this model predicts no extra x-ray diffraction lines (see Table III of Ok and Mullen's first paper) whereas the determination of a monoclinic space group for antiferromagnetically ordered CoO, which we have used in our group-theoretical analysis, relied on the appearance of some extra x-ray lines (see Fig. 3 of Saito *et al.*[8]) that would not appear if there were no distortion.

ACKNOWLEDGMENTS

The authors are grateful to the Plessey Co. for financial support of the experimental work reported here, and to Professor R. Loudon for helpful discussions.

[27] J. Kanamori, in *Magnetism*, edited by G. T. Rado and H. Suhl (Academic Press Inc., New York, 1963), Vol. I, p. 196.
[28] H. N. Ok and J. G. Mullen, Phys. Rev. **168**, 550 (1968); **168**, 563 (1968).